Dynamic Regime Electromagnetic Torque in Brushless Direct Current Motors

Ion Vlad, Sorin Enache, Monica Adela Enache
University of Craiova, Faculty of Electrical Engineering, Craiova, Romania
ivlad@em.ucv.ro, senache@em.ucv.ro, menache@em.ucv.ro

Abstract - **This study aimed at establishing the mathematical model for determining the dynamic regime torque and at emphasizing constructive aspects which influence its magnitude and variation. Brushless direct current motors are very present and there have been carried out researches regarding their design and optimum construction. The technology evolution in several areas has caused an increase in production of permanent-magnet BLDC motors, which has good technical-economic performances for a large range of controlled-speed applications. The study carried out, by the simulations we presented, shows that these motors have high torque oscillations in a complete rotation. There are identified the slots which create high torques, respectively low torques, in a complete rotation, thus justifying the oscillations. In this paper there is emphasized that the optimum variant of maximum torque involves a supply by six pulses per period in direct direction, also indicating the value of the control angle. The most unfavourable variant occurs at brushless direct current motor supplied by three pulses per period and reverse succession of phases, where the average value of the torque decreases by 56.7% over the optimum machine. A complete elimination of oscillations in this type of motor is not possible, but an optimal design can reduce them considerably.**

Keywords*: brushless direct current motor, design, simulation, optimization.*

I. Introduction

Classical direct current motors are replaced by brushless direct current motors in several applications due to low energy consumption, their high reliability and low maintenance. The main advantage of this motor is high specific power obtained by means of rare-earth permanent magnets, so a much decreased weight [1-5].

The possibility to replace the assembly comutator-brushes of direct current motor by a contactless commutation device emphasized the advantages of this machine [6-10].

For electrical devices and installations supplied by local energy sources, it is advisable to use permanent-magnet direct current fractional-horsepower motors which have a low weight per unit of power, high efficiency, linear mechanical characteristic, very high rotating speeds; they are noiseless motors, with safe operation, without monitoring and maintenance etc.

The motors used for two-wheeler vehicles (electrical scooter, electrical bicycle, electrical motor-scooter) are permanent-magnet direct current motors manufactured with ”brushless” technology.

Brushless direct current motors are used in peripheric equipments of computers, in potentiometers with motor and in devices following advance of copying machines [3], [6], [11-14]. There is experienced using brushless direct current motors rated at high power, in electrical cars and auto-trucks.

At present [13], [15], [16-19], there are fabricated magnetic materials with special features, being possible to carry out brushless permanent-magnet direct current motors rated at low and middle powers.

In order to simplify the scheme of the commutation device and to reduce its cost, an armature winding having a minimum number of coils is used in these motors.

II. Construction and Operation

The motor construction uses permanent magnets made of rare earths [7], [16-19]. Good perspectives have the materials of type Nd-Fe-B, which have good magnetic features, are less breakable and have a low cost (much less than the magnets of type Sm-Co), but have a low operation temperature (80-100)^{o}C. The temperature has an important effect upon the magnet characteristics, so upon the motor characteristics.

High currents and high temperatures cause demagnetization. In case of drives using brushless direct current motors, demagnetization is not a problem because the current is permanently followed and it is limited by controller and measuring motor temperature is a simple problem.

Brushless direct current motors are now frequently used for two-wheeler vehicles. They are carried out as a close construction IP 44, are assembled in the very wheel hub, have a solid construction, facing shocks, vibrations, bad weather. The producer pays a special attention to aspect and operation because the motor is integrated in the hub of the back wheel and the battery accumulator and the display have low dimensions.

Modern computation tools have enabled the capitalization of complex mathematical models for investigating and computing the electromagnetic torque of such motors.

An important aspect is the *functional criterion*, meaning to carry out the motor with certain technical characteristics imposed by customer, these being defined by means of the parameters: resistances, inductances, inertia moment, steady state and transient time constants etc. These parameters depend upon geometry, construction and electromagnetic stresses of the machine. In these circumstances, the theme we approached in this paper is a subject of interest for engineering.

III. Mathematical Model for Establishing Dynamic Regime Electromagnetic Torque

The mathematical model carried out for establishing instantaneous values of electromagnetic torque [3], [4], [6], [8-9] is based on relations known in literature. The study we have carried out and presented below has considered:

$$\beta = p \cdot \alpha + \gamma \tag{1}$$

α - geometrical angle corresponding to the rotor displacement Fig.1, β -control angle of the a-phase current, γ -delay angle for the control of the current I_a.

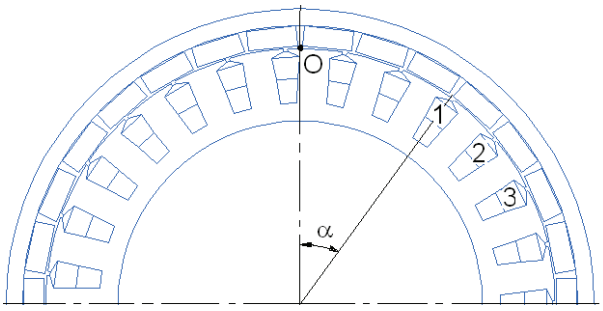

Fig.1. Cross-section through the motor.

There has been established the space origin in the point O, (α =0 –neutral axis, Fig. 1) and the lines of the magnetic field have been modelled as follows: the opposite armature has been taken as being smooth (the slot opening is very small) and it has been considered that the field lines are radial over the whole magnet width, while they are modelled by arcs and segments outside that area.

The design data of the motor provide the magnetic voltage of the air-gap and its size in the magnet zone. In crossing points (ferromagnetic core-air) where the tangential component of magnetic induction preserves, there has been imposed the condition of continuity and derivability of the curve modelling the field line.

The air space between the magnets b_{0mg}, makes the air-gap size variable at the armature periphery, thus modelling the distribution curve of the air-gap magnetic induction (Fig.2), with a polynom-function of the third degree where continuity and derivative conditions have been imposed.

This way, we have modelled numerically the air-gap magnetic induction relatively to the rotor position:

$$B = f(\alpha) \tag{2}$$

and, by using this relation, there has been simulated the curve of air-gap magnetic induction, Fig. 2.

The armature winding is in star connection, distributed in slots (on tooth). The armature winding is radial, star connection, distributed in two layers into slots, with the pitch y=1 (on tooth).

According to literature, for having a high rotating torque, during the operation we will have two coils connected in series and the third one at rest. Consequently, there are rectangular alternating currents, the duration of a pulse is of 120 electrical degrees.

There has been established the time origin t=0 when α= 0 and there has obtained the numerical modelling of currents relatively to the rotor position and the currents control:

$$I_a, I_b, I_c = f(\alpha, \gamma) \tag{3}$$

The control device models, on a polar pitch, the three currents of the windings relatively to β -electrical angle. The phase currents b and c are displaced in phase by 120 electrical degrees.

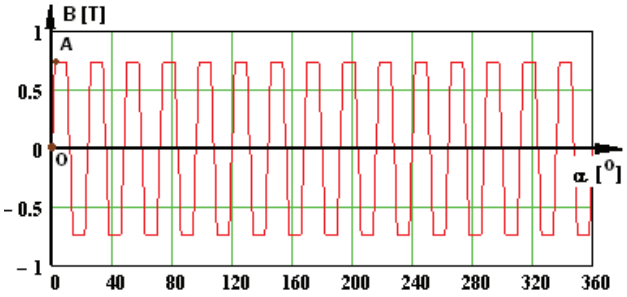

Fig.2. Distribution curve of air-gap magnetic induction on the whole machine.

It is considered that the point O –the space origin, is on the axis of the first slot, taken as a reference. Consequently, the position of the slot N_{cx} is established by the geometrical angle as below:

$$\zeta_{Ncx} = \alpha + \frac{360}{N_c} N_{cx} \tag{4}$$

There has been computed the ampere-turns corresponding to the conductors placed in the upper layer crossed by the current I_x, respectively to the conductors placed in the under layer where we have the current I_y for each slot:

$$\theta_{Ncx} = 0.5 \cdot n_c I_x + 0.5 \cdot n_c I_y \tag{5}$$

where we have: n_c –number of conductors/slot, N_{cx} – number of slot, I_x, I_y are the currents I_a, I_b or I_c relatively to the slots distribution on zones and phases, carried out according to literature.

There are considered the conductors and the afferent ampere-turns concentrated in the slot axis and at the air-gap level:

$$\theta_{Ncx} = f(\alpha, \gamma, N_{cx}) \tag{6}$$

In this stage there are known the air-gap magnetic induction $B(\alpha)$, the ampere-turns of each slot $\theta_{Ncx}(\alpha, \gamma, N_{cx})$, the iron length l_{Fe}, so it is possible to compute the torques determined by each slot with the relation:

$$T_{Ncx} = 0.5 \cdot D \cdot B(\alpha) \cdot \theta(\alpha, \gamma, N_{cx}) \cdot l_{Fe} \tag{7}$$

This way, we have modelled numerically the electromagnetic torque of a slot:

$$T_{Ncx} = f(\alpha, \gamma, N_{cx}) \tag{8}$$

For the total torque we have:

$$T = \sum_{i=1}^{N_c} T_{Ncx} \tag{9}$$

On the basis of the mathematical model presented, it is possible to carry out a computation program, where N_p – number of points per a complete rotation and N_{pi} – number of points by which the control is delayed, per a pole pair. This way, elementary angles result:

$$\alpha_e = k_p \frac{360}{N_p} \qquad k_p = 1,2,3..., N_p \tag{10}$$

$$\gamma_e = k_{pi} \frac{360}{N_{pi}} \qquad k_{pi} = 1,2,3..., N_{pi} \tag{11}$$

For values assigned to N_p and N_{pi} there are computed and memorized the instantaneous values and the average value in a complete rotation of torque given by a slot, respectively the total average torque.

IV. Results, Simulations and Conclusions

Using the mathematical model presented before and advanced numerical computation methods [20-24], there have been carried out simulations and, with the results obtained, there have been pointed out conclusions regarding electromagnetic torque of the motor.

All the results we have obtained and the simulations presented here are emphasized by a concrete example of permanent-magnet brushless direct current motor. The motor is rated as follows: P_N=100 W; U_N= 20 V; I_N=6.0 A, n_N= 450 r/min, and is built with 27 slots, 2p=30 magnetic poles of type Nd-Fe-B.

A.1. Supply by six pulses per a pair of poles and direct succession of phases

The control device, which supply the motor, sets the phase current for three phases (Table I), during an operation period.

Table I.
The matrix of the three phase currents

α [°] el.	0÷60	60÷120	120÷180	180÷240	240÷300	300÷360
I_a [A]	I_N	I_N	0	- I_N	- I_N	0
I_b [A]	- I_N	0	I_N	I_N	0	- I_N
I_c [A]	0	- I_N	- I_N	0	I_N	I_N

For criterion "maximum electromagnetic torque" the optimum variant of winding has been found, where the distribution of slots per zones and phases is that presented in Table II. Because we have three overlapped stars, there have been presented the ampere-turns produced by currents which cross the conductors from the nine slots.

Table II.
Slot ampere-turns

Slot no.	1	2	3	4	5	6	7	8	9
Ampere-turn in the upper layer	θ_A	$-\theta_A$	$-\theta_B$	θ_B	$-\theta_B$	$-\theta_C$	θ_C	$-\theta_C$	$-\theta_A$
Ampere-turn in the lower layer	θ_A	$-\theta_A$	θ_A	θ_B	$-\theta_B$	θ_B	θ_C	$-\theta_C$	θ_C

In Fig.3 there is presented the curve of the electromagnetic torque average value, for a complete rotation, for different control angles of currents.

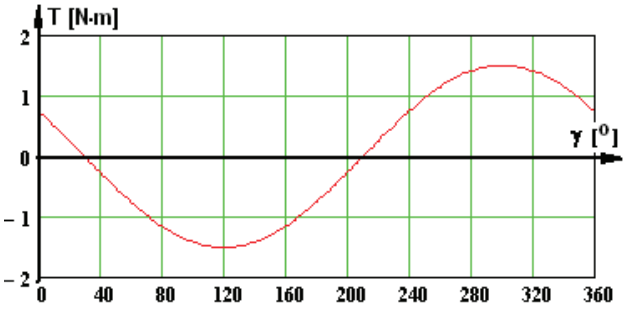

Fig.3. Torque average value at a complete rotation for different control angles of currents.

In order to obtain a maximum torque for a complete rotation, the control electrical angle is γ=294° or the geometrical angle ξ=294/15=19.6° shows where the first position transducer is placed on the rotor (fixed armature) relatively to the origin –point O, in the rotation direction. The next positions where the transducers are placed are at 120° electrical degrees in the rotation direction.

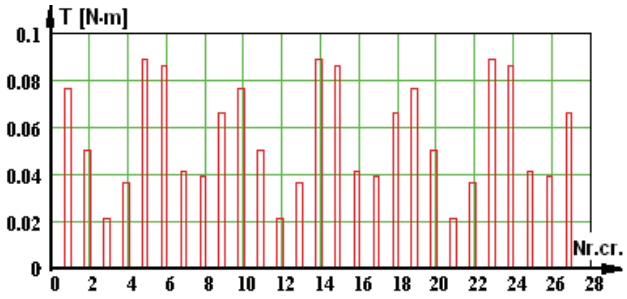

Fig.4. Torque values relatively to the number of slot.

For the angle γ -fixed and (α= 0 ÷ 360°), by means of the program there have been computed the average value of the torques given by the currents which cross the conductors from the armature slots. The total torque of the motor has resulted as T_N=1.52 N·m, for a speed of n_N=450 r/min, so, the useful mechanical power results as P_2=72.2 W.

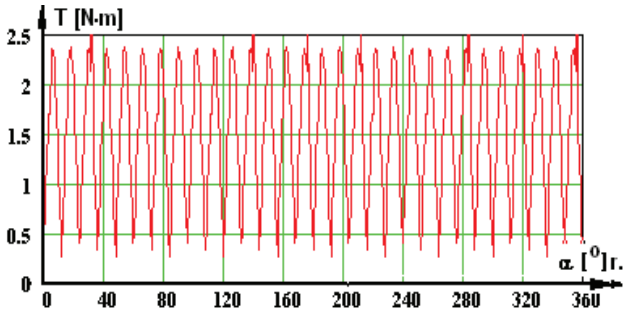

Fig.5. Variation curve of the motor torque at a complete rotation.

By analyzing Fig.4, we notice the slots and their contribution at producing the motor torque: 5, 6, 14, 15, 23, 24 –very important slots, 1, 10, 14 –important slots, 4, 8, 13, 22 –slots with mild torques, 3, 12, 21 –slots with low torques.

In Fig.5 we can see how the total torque of brushless direct current motor modifies for a complete rotation (a lot of peaks and variations within large limits).

There are presented below the torque variation curves, for a complete rotation, at different slots, Fig. 6.

From the analysis of these figures we notice that, at slots 3, 12, 21 the average value of the torque is very low and the torque has large positive and negative oscillations and slots 5, 6, 14, 15, 23, 24 provide high torques.

Periodical oscillations of torque are a major cause of vibrations, which in some cases can produce the mechanical resonance of the system.

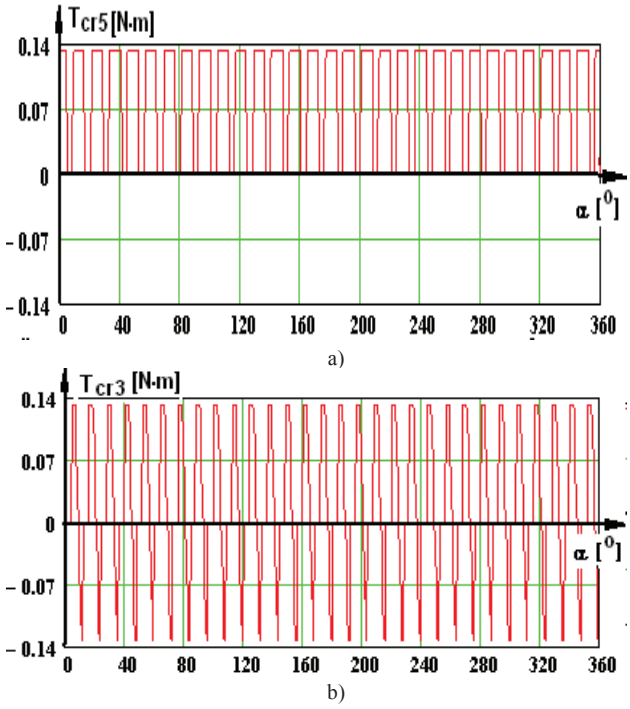

Fig.6. Variation curves of torques for a complete rotation: a) provided by the currents which cross the conductors from the slot 5; b) for the slot 3.

A.2. Supply by six pulses per a pair of poles and reverse succession of phases

In the matrix of the three phase currents from table no. 1, the phases b and c are reversed during a period.

The curve of the average value of the electromagnetic torque for a complete rotation, for different control angles of currents is presented in Fig.7.

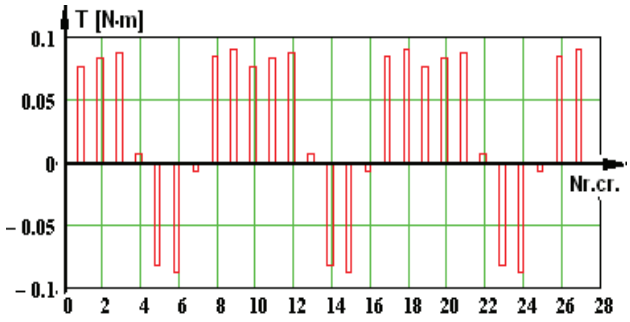

Fig.7. Values of torques relatively to the slot number.

For the electrical angle γ=10 and (α= 0 ÷ 360°), by means of the program, there have been computed the average values of the torques provided by the currents which cross the conductors from the armature slots.

The total torque of the motor has resulted as T_N=0.755 N·m, at a speed of n_N=450 r/min, so the useful power is P_2=35.3 W.

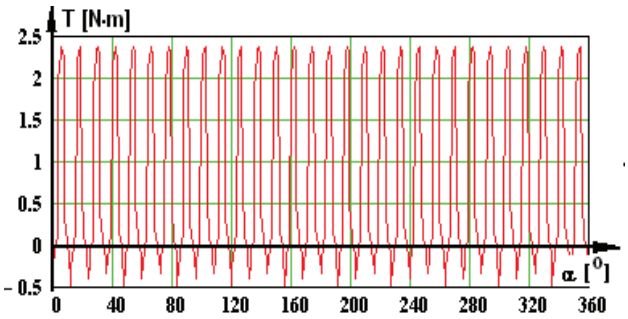

Fig.8. Variation curve of the motor torque for a complete rotation.

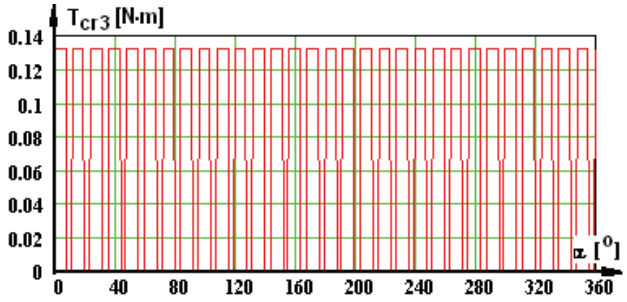

Fig.9. Variation curve of torque for the slot 3 for a complete rotation.

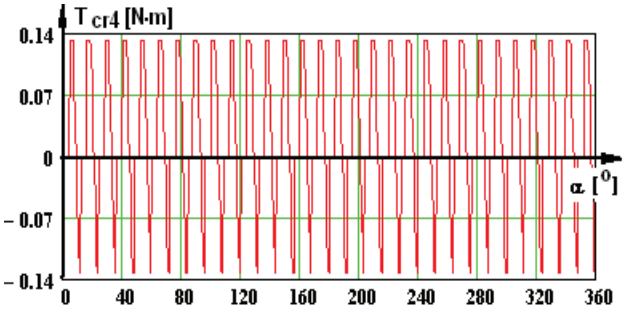

Fig.10. Variation curve of torque in a complete rotation for the slot no. 4.

The most important slots are multiple of three, with an average torque of T_{cr3}=0.084 N·m, and the representative torque is presented in Fig.9. The slot no. 4 causes a torque having very high oscillations (positive and negative), Fig.10, the average value being T_{cr4}=0.012 N·m.

B.1. Supply by three pulses per a pair of poles and normal succession of phases

The values of the three phase currents during a period are given by a three-pulse control device. The program of numerical computation enables this analysis which, on the basis of the simulations we carried out and the results we obtained, shows how many drawbacks this supply variant has. The matrix of the three phase currents (table no. 3), during a period is given by a three pulses control device.

TABLE III.
The matrix of the three phase currents

α [°] el.	0÷60	60÷120	120÷180	180÷240	240÷300	300÷360
I_a [A]	I_N	I_N	0	0	- I_N	- I_N
I_b [A]	- I_N	- I_N	I_N	I_N	0	0
I_c [A]	0	0	- I_N	- I_N	I_N	I_N

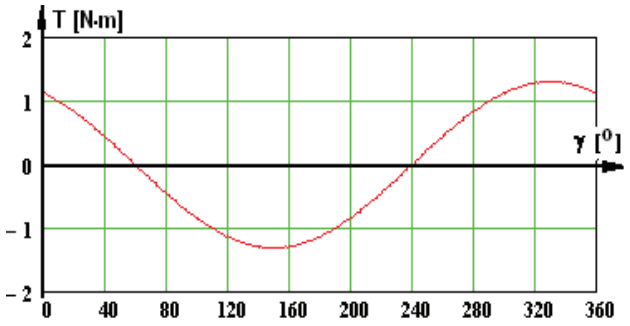

Fig.11. Average value of torque at a complete rotation for different control angles of currents.

For different control angles of currents there is obtained the curve of the electromagnetic torque for a complete rotation, Fig.11. There results two maximum torques, a positive one for γ=330 electrical degrees and a negative one for γ=150 electrical degrees.

Corresponding to the control angle γ=330° and α= 0 ÷ 360°, there have been established the torques provided by the currents which cross the conductors from the armature slots.

The total torque of the motor has resulted as T_N=1.314 N·m, for a speed of n_N=450 r/min, so we have a useful power of P_2=61.9 W.

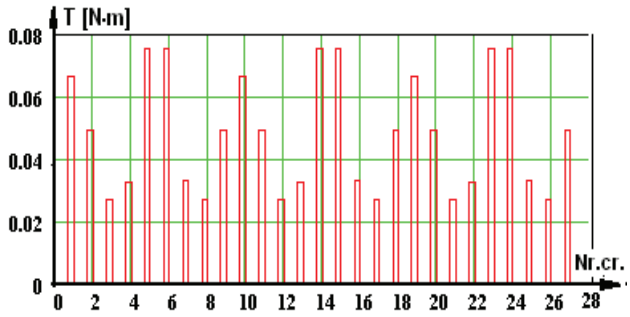

Fig.12. Torque values relatively to the slot number.

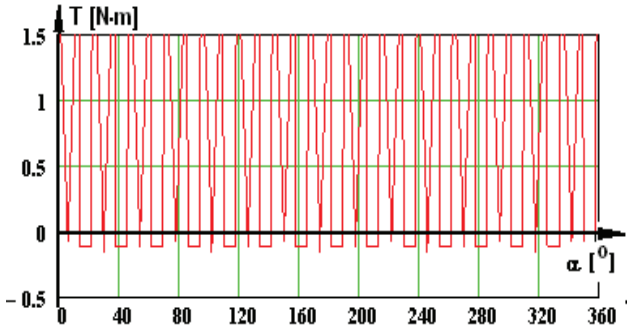

Fig.13. Variation curve of the motor torque for a complete rotation.

In Fig. 12 there can be seen the curve of the total torque, for a complete rotation (a lot of peaks and variations within large limits).

B.2. Supply by three pulses on a pair of poles and reverse succession of phases

There are preserved three pulses on a period but there are interchanged the phases b and c. There is simulated the curve of the electromagnetic torque for different control angles of currents.

There result two maximum torques, a positive one for γ=30 electrical degrees and a negative one for γ=210° electrical degrees. For the control angle γ=30° and α= 0 ÷ 360°, there have been computed the torques provided by the currents which cross the conductors from the armature slots, Fig.14.

There resulted a total average torque of T_N=0.657 N·m, for a speed of n_N=450 r/min, so we have a useful power of P_2=30.96 W.

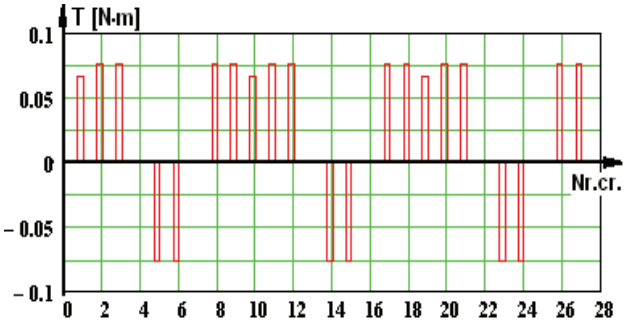

Fig.14. Torque values relatively to the slot number.

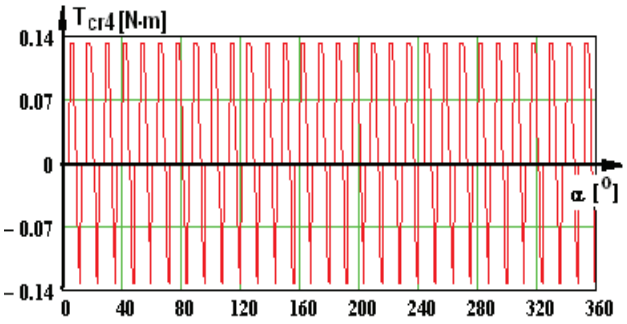

Fig.15. Variation curve of total torque in a complete rotation.

In this case, Fig.15, the torque has very high oscillations (positive and negative) and the average value is lower T_N=0.657 N·m.

The most important results of the study we have carried out are filled in table no. 4, where: T_{med} –average value of the torque for a complete rotation, $T_{cr.max}$, $T_{cr.min}$ –minimum/maximum value of the slot torque, N_{crt} with T>0/<0 –number of slots which provide positive/negative torque.

Table IV.
Couples notches created by the rotor

	Supply by six pulses per period		Supply by three pulses per period	
	Succession a, b, c	Succession a, c, b	Succession a, b, c	Succession a, c, b
T_{med} [Nm]	1.52	0.755	1.314	0.657
$T_{cr.max}$ [Nm]	0.084	0.092	0.076	0.075
$T_{cr.min}$ [Nm]	0.021	0.007	0.026	0.063
Nr_{crt}. cu T>0	27	21	27	15
Nr_{crt}. cu T<0	0	6	0	6

V. CONCLUSIONS

A constant wave of torque is important, especially in servo-drives, where a high precision, a control of speed and rotor position are required. For instance, in tool-machines, finishing the processed piece is negatively affected by torque oscillations of driving motor. Periodical torque oscillations or *ripple* are, in a lot of situations, the cause of vibrations which are annoying when mechanical resonance occurs in equipment structure.

The study we have carried out and the results presented in table no.4 recommend the supply by six pulses and direct succession of phases, because there results the highest torque for a complete rotation, all the slots are active and provide positive torques, so the oscillations are lower.

We can notice that in all these cases we have some very active slots (T_{cr}=0.084 N·m) and some almost inactive slots (T_{cr}=0.021 N·m). The most unfavourable variant is the supply by three pulses and reverse succession of phases, when the torque gets high oscillations and decreases to 56.7% over the torque corresponding to the optimum variant.

An almost constant torque cannot be obtained for brushless direct current motor, but we can draw near this requirement. The inertia moment of the rotor and the high speed decrease the speed oscillations caused by torque oscillations. A performing control system, with a reaction loop by speed, can reduce considerably the torque oscillations for low speed, too, if the amplification and the bandwidth are high enough.

ACKNOWLEDGMENT

This paper was realized under the frame of the grant POC-A1-A1.2.3-G-2015 ID 40 401.

Received on July 17, 2016
Editorial Approval on November 24, 2016

REFERENCES

[1] C. Bianchini, F. Immovilli, E. Lorenzani, A. Bellini, M. Davoli, "Review of Design Solutions for Internal Permanent Magnet Machines Cogging Torque Reduction", 2011, *IEEE Transactions on Magnetics*, vol. 48, no.10, Oct. 2012, pp 2685-2693.

[2] A. Campeanu, I. Vlad, S. Enache, "Numerical Analysis of the Dynamic Behavior of a High Power Salient Pole Synchronous Machine by using a Corrected Model", AECE Journal, Vol.12, Issue 1, Year 2012, pp.97-102.

[3] L. Dosiek, P. Pillay, "Cogging Torque Reduction in Permanent Magnet Machines", IEEE Trans. On Industry Applications, vol. 43, no. 6, 2007, pp 1565-1571.

[4] W. Fei, P.C.K. Luk, "A New Technique of cogging Torque Supperssion in Direct-Drive Permanent-Magnet Brushless Machines", IEEE Trans. on Industry Applications, vol 46, no. 4, July/Aug. 2010, pp. 1332-1340.

[5] M.S. Islam, S. Mir, T. Sebastian, "Issues in reducing the cogging torque of mass-produced permanent magnet brushless DC motor", IEEE Trans. on Industry Applications, vol. 40, no. 3, 2004, pp.813 – 820.

[6] J. Kaňuch, Z. Ferková, "Design and simulation of disk stepper motor with permanent magnets", Archives of Electrical Engineering, vol. 62, no. 2 (2013), pp. 281-288.

[7] T. Koch, A. Binder, "Permanent magnet machines with fractional slot winding for electric traction", International Conference on Electrical Machines, ICEM 2002, Brugge, Belgien, 2002.

[8] M. Miyamasu, K. Akatsu, "Efficiency Comparison between Brushless DC Motor and Brushless AC Motor Considering Driving Method and Machine Design", IEEE Industrial-Electronics-Society (IECON 2011), 2011, pp.1830-1835.

[9] I. Vlad, S. Enache, M.A. Enache, "Optimization of Low-Power Brushless Direct Current Motors", The 9 th International Symposium on ADVANCED TOPICS IN ELECTRICAL ENGINEERING, 7-9 mai 2015, Bucureşti, pp.176-181.

[10] I. Vlad, S. Enache, L. Mandache, M.A. Monica, "Transversal Shape Optimization of a Brushless DC Motor for Electric Vehicles", Annals of the University of Craiova, Electrical Enginnering series, nr. 39, Anul 2015, pp.144-149.

[11] T. Sebastian, S. Mir, M. Islam, "Electric Motors for Automotive Applications", EPE Journal, vol. 14, no.1, 2004, p.31-37.

[12] T. Tudorache, L. Melcescu, M. Popescu, "Methods for Cogging Torque Reduction of Directly Driven PM Wind Generators", 12th International Conference on Optimization of Electrical and Electronic Equipment, OPTIM, 2010.

[13] S.H. Zareh, M. Khosroshahi, M. Abbasi, K.G. Osgouie, "The select of a permanent magnet brushed DC motor with optimal controller for providing propellant of a Home Mobile Robot", IEEE (ICMA), 2010, pp.1137 – 1141.

[14] Y.L. Zhang, W. Hua, M. Cheng, G. Zhang, X. F. Fu, "Static Characteristic of a Novel Stator Surface-Mounted Permanent Magnet Machine for Brushless DC Drives", 38th Annual Conference on IEEE-Industrial-Electronics-Society (IECON 2012), 2012, pp.4139-4144.

[15] N. Vasile, V. Dogaru, C. Sălişteanu, Electrical machines. Construction, technology and special applications, ICPE Publishing House, Bucuresti, 2000 (in Romanian).

[16] *** Catalog ICPE Bucharest, Sintered magnets Al-Ni-Co and Nd-Fe-B –magnetic characteristics.

[17] http://neomagnet.ro/produse-in-stoc/D165_H15_mm_magnet_inel_ sm2co17.

[18] http://www.icpe-me.ro/motoare_magneti_permanenti.ht

[19] http://www.et.upt.ro/admin/tmpfile/ fileM1369636748file51a2ff8c8b180.pdf

[20] O. Cira, *Lessons of MathCad*, The Blue Publishing House, Cluj-Napoca, 2000 (in Romanian).

[21] I. Daniel, I. Munteanu, *Numerical methods in electrical engineering*. Bucharest, MATRIX ROM Publishing House, 2004 (in Romanian).

[22] V. Fireţeanu, M. Popa, T. Tudorache, *Numerical modeling in the study and design of electrical devices,* Editura Matrix Rom, Bucuresti, 2004 (in Romanian).

[23] St. Nagy, *Numerical modelling of electromagnetic and thermic field*, Applications, Oradea 2004 (in Romanian).

[24] P. Năslău, R. Negrea, s.a., *Computer aided mathematics*, Timişoara, Politehnica Publishing House, 2005 (in Romanian).